Supporting Online Material for

Fast Vesicle Fusion in Living Cells Requires at Least Three SNARE Complexes

Ralf Mohrmann,* Heidi de Wit, Matthijs Verhage, Erwin Neher, Jakob B. Sørensen*

*To whom correspondence should be addressed. E-mail: Ralf.Mohrmann@uks.de (R.M.); jakobbs@sund.ku.dk (J.B.S.)

Published 16 September 2010 on *Science* Express
DOI: 10.1126/science.1193134

This PDF file includes:

Supporting Online Material

Materials and methods

Chromaffin cell preparation and viral expression system. *Snap-25* null embryos were obtained by Cesarean section at E17-E18. Preparation of adrenal glands and cultivation of chromaffin cells were performed as described before (*S1*). Plasmids needed for generation of Semliki Forest viruses were generated by standard techniques of molecular biology. Starting from a cDNA encoding an N-terminal fusion construct between SNAP-25 and EGFP (*S2*) (here denoted EGFP-SN25B), we generated GFP-SN25B variants with either single (M71A or I192A) or double alanine substitutions in layer +5 by PCR mutagenesis. The generated PCR-fragments were cloned into a modified pSFV1 plasmid containing a multiple cloning site with unique Nsi I and BssH II restriction sites (courtesy of Ralf B. Nehring). To obtain mCherry-tagged versions of these SNAP-25 variants, appropriate PCR fragments of mCherry (*S3*) (mCh; kind gift of Dr. Roger Tsien) and mutated SN25B were generated, fused by PCR, and cloned into pSFV1 plasmid. Bicistronic expression units were constructed by fusing PCR-fragments of the polio virus-IRES sequence or the CITE-IRES sequence to PCR-fragments containing EGFP-SN25B or mCherry-SN25B M71A, I192A. The polio virus IRES sequence was adapted from an existing SFV transfer vector previously generated in our lab (*S4*). The EMCV IRES sequence was taken from pCITE2a (Novagen/Merck, Nottingham, UK) and further modified according to (*S5*) to yield attenuated versions. In an initial step of the cloning strategy we generated a fused PCR product containing the appropriate IRES sequence and the second open-reading frame either containing EGFP-SN25B or mCh-SN25BL5**. Care was taken to place the start-codon of the sequence at the right position with respect to the end of the IRES sequence. Due to a lack of restriction sites the generated PCR product was then fused to a fragment covering the downstream sequence of pSFV1 up to the

unique Spe I site. The resulting PCR product was finally inserted back into pSFV1 using the restriction sites BssH II and Spe I. In a second step an additional PCR fragment containing the sequence of the appropriate first open reading frame was generated and cloned into the modified pSFV1 vector using the restriction sites Nsi I and BssH II. All constructs were thoroughly sequenced before production of SFV particles. For experiments stored virus aliquots were activated by chymotrypsin cleavage, chymotrypsin was inactivated with aprotinin, and chromaffin cells were infected at days 2–4 after isolation. Electrophysiological recordings were performed at room temperature 5-8 h after infection with viruses.

Expression assays by Western blot and fluorescence intensity. The expression of tagged SNAP-25 variants after infection with bicistronic Semliki Forest viruses (SFV) was analyzed by Western blot and fluorescence intensity measurements. Cultured bovine chromaffin cells were prepared, infected, and subjected to Western blot analysis as described before (*S6*). Protein lysates were prepared under non-reducing conditions to allow for the formation of disulfide bonds, which results in characteristic band-shifts for GFP-tagged and mCherry-tagged SNAP-25 protein. Protein samples (30µg) were separated on 4-20% polyacrylamide-gels (Ready Gel; Bio-Rad Laboratories, Hercules, CA) and transferred onto nitrocellulose membranes (Amersham Hybond-ECL; GE Healthcare Bio-Sciences, Uppsala, Sweden). After protein transfer, the blot was cut at ~70kDA, and SNAP-25 variants were assayed with polyclonal anti-SNAP-25 (1:3,000, Synaptic Systems, Göttingen, Germany) on the lower molecular weight section of the blot. On the other part of the blot valosin–containing protein (VCP) served as loading control and was detected by monoclonal anti-VCP (1:3,000, Abcam, Cambridge, United Kingdom). Protein bands were visualized by chemoluminescence using an ECL detection kit

(SuperSignal, West Pico; Pierce Chemical, Rockford, IL). Quantification was done by densitometry using ImageJ software (National Institutes of Health, Bethesda, Maryland). The relative expression levels of both SNAP-25 variants were calculated from the band intensities of the characteristic, oxidized protein species. Note that the ratio of oxidized to reduced protein for both, GFP-SNAP-25 and mCh-SNAP-25, was constant under the used experimental conditions, and was determined in separate experiments. To obtain an estimate of the fraction [mCh-SNAP-25]/([mCh-SNAP-25]+[GFP-SNAP-25]) by fluorescence intensity measurements, we took microphotographs of infected bovine chromaffin cells just before preparing lysates for western blot analysis. Using appropriate filtersets we obtained pictures of GFP- and mCherry fluorescence at a fixed exposure time (8s). The intensities of GFP and mCherry fluorescence were quantified in randomly selected chromaffin cells (150-450 cells). A GFP-mCherry fusion protein was used as reference for the calculation of the relative expression of mCherry-tagged and GFP-tagged SNAP-25, as the fusion protein presents both fluorophors at a fixed ratio of 1:1.

Electrophysiology, electrochemistry, and calcium imaging. Flash photolysis of caged calcium, ratiometric measurements of intracellular calcium concentration, patch-clamp capacitance measurements, and amperometric recordings were performed as previously described (*S1, S7*). Secretion was elicited by flash photorelease of caged calcium and monitored in parallel by capacitance measurements and amperometric recordings, which ensured that mainly catecholamine release from dense-core vesicles was studied. To eliminate photo-artifacts from amperometric traces originating from the UV flash light, isolated artifacts were recorded after removal of the chromaffin cell using the patch pipette and subsequently subtracted from associated traces. Nitrophenyl-EGTA (NPE) used in calcium-uncaging experiments was obtained from Synaptic Systems (Göttingen, Germany).

Intracellular calcium concentrations were determined with two dyes (fura-4F and furaptra, Invitrogen) as described in earlier studies (Voets, 2000; Sørensen et al., 2002). Unlike previous studies, Vitamin C was added to the intracellular solution to minimize flash-induced damage to fura dyes. Fura-dyes were excited at 340nm and 370nm for ratiometric calcium determination. The composition of the intracellular solution was (in mM): 100 Cs-gluconate, 8 NaCl, 4 $CaCl_2$, 32 HEPES, 2 Mg-ATP, 0.3 GTP, 5 NPE, 0.4 fura-4F, 0.4 furaptra, and 1 Vitamin C, pH 7.2 (osmolarity was adjusted to 290 mOsm). The extracellular solution was (in mM): 145 NaCl, 2.8 KCl, 2 $CaCl_2$, 1 $MgCl_2$, 10 HEPES, pH 7.2 (osmolarity was adjusted to 300 mOsm). Data were analyzed using Igor Pro 6 software (Wavemetrics, Lake Oswego, OR). Analysis of release kinetic was performed by fitting capacitance traces with the sum of three exponential functions. As described earlier (*S1*), this approach allowed the distinction of the two burst components (denoted as 'fast burst' and 'slow burst' in the figures) and the quantification of their corresponding amplitudes and time constants (referred to as amplitudes A_{fast} and A_{slow} and time constants τ_{fast} and τ_{slow}). The third exponential is used for fitting the sustained component. If the fit identified a negative amplitude of at least one component, or if two time constants were closer than a factor two apart, fitting with a two exponential function (one exponential for the burst, one for the sustained component) was used instead. Time constants faster (smaller) than 50 ms were interpreted to describe release from the readily-releasable pool, while time constants between 50 and 500 ms were considered to represent fusion of vesicles from the slowly-releasable pool. It should be noted that some of our results indicate significant changes of both burst time constants, which indicates that both release processes are changed. In this case, a clean distinction of the two burst components (fast and slow) is not always possible. Results are generally given as mean±SEM in figures. If not marked otherwise, student's t-test (unpaired) was used for statistical comparisons.

Quantification of expression levels by intensity measurements in single cells. The relative expression ratios of mCh-SN25BL5** and EGFP-SN25B were determined by wide-field fluorescence intensity measurements within individual chromaffin cells right before electrophysiological recordings. Fluorophors were excited at appropriate wavelengths (mCh: 545 nm; EGFP: 475 nm) using a monochromator as lightsource (Polychrome II; Till Photonics, Gräfelfing, Germany). Fluorescence pictures were taken with an Imago CCD camera (Till Photonics) using matching dichroic mirrors (EGFP: HC Beamsplitter BS495; mCh: Q570LP) and emission filters (EGFP: HQ525/50m; mCh: HQ610/75M; all supplied by AHF Analysentechnik, Tübingen, Germany). Additional excitation filters (EGFP: HQ470/40; mCh: 545/30; AHF Analysentechnik, Tübingen) were used to suppress background white light emitted by the monochromator. Using this optical setup crosstalk between channels was estimated to be 1.5±0.5% for EGFP fluorescence in the mCherry channel and 0.6±0.2% for mCherry fluorescence in the GFP channel. Pictures were analyzed with TillVision 4.0 software (Till Photonics, Gräfelfing, Germany). Since viral expression caused accumulation of SNAP-25 protein within intracellular compartments, we restricted our analysis to regions extending 1-2 µm from the plasmamembrane. A virally expressed EGFP-mCherry fusion protein was employed to define a reference point with equimolar fluorophor ratio under our experimental conditions. Using this reference we calculated the fraction [mCh-SN25BL5**]/([mCh-SN25BL5**] +[EGFP-SN25B]) for each cell.

Colocalization of protein variants by confocal microscopy. Distribution patterns of mCh-SN25BL5** and EGFP-SN25B in chromaffin cells were studied using a confocal laser scanning microscope (LSM 710, Carl Zeiss Microimaging GmbH, Germany). Cultured mouse chromaffin cells were infected with bicistronic SFV mCh-SN25BL5** IRES EGFP-SN25B and imaged 5-6 h post

infection. Confocal sections of 0.8-0.9 µm (pinhole 1 Airy unit) were taken slightly above the foot area of each cells. EGFP and mCherry were excited at 488 nm and 543 nm, respectively. Images of EGFP and mCherry fluorescence were acquired sequentially with alternating laser excitation and separate channels using recommended detector presets for EGFP and mCherry (ZEN 2008 software, Carl Zeiss Microimaging GmbH). Detector gains of both channels were individually adjusted to cover the whole intensity range. Eight frames were taken in each channel in an alternating fashion and averaged to yield the final image. Only cells with moderate expression of both SNAP-25 variants were selected for analysis, as overly high expression levels lead to an almost homogenous protein distribution in cells. Image analysis was performed with ImageJ software. Using the popular "Just Another Colocalisation Plugin" (JACoP; (*S8*)) we analyzed the extent of colocalization between mCh-SN25BL5** and EGFP-SN25B. As reference we used the EGFP-mCh fusion protein, which by definition is expected to produce highly colocalized fluorescence signals. Crosstalk between channels under these experimental conditions was tested by imaging cells solely expressing EGFP or mCh-tagged SNAP-25. Using fixed gain settings for both detector channels we found 4.1±0.9% (n=18) crosstalk for EGFP in the mCh-channel and 1.1±0.2% (n=18) crosstalk for mCh in the EGFP-channel, respectively. Note that crosstalk of EGFP in the mCh-channel was likely overestimated in this control experiment due to the gain settings that favored the red channel over the green as well as due to the occurrence of background fluorescence.

Amperometric spikes. Amperometric spikes were recorded as previously described (*S1*). While amperometric recordings were performed with carbon fibers of 10 µm (Amoco Corp., Greenville, SC) during flash-photolysis experiments, we employed fibers of 5 µm diameter for recordings of single spikes in order to reduce noise. Due to a rapid ageing of the amperometric electrodes, we used freshly

prepared fibers for no more than two consecutive recordings. Fibers were clamped to +720mV, and amperometric current signals were amplified and prefiltered at 3 kHz using an EPC-7 (HEKA Elektronik, Lambrecht/Pfalz, Germany). For further analysis current traces were digitally filtered at 600 Hz (Gaussian filter) in Igor Pro. Amperometric spikes were detected (threshold 5pA) and analyzed with regard to amplitude, rise-time, halfwidth, and pre-spike foot duration/charge using a custom macro running in Igor Pro. To account for the significant cell-to-cell variability of amperometric data, and the fact that parameters are often not normally distributed, we relied on the cell median instead of the mean for our analysis. The medians of the waveform parameters were determined for each individual cell based on all recorded spikes, and the calculated medians were subsequently averaged within the experimental group and statistically compared. To ensure a sound estimation of the median only recordings with at least ten spikes were included in the analysis.

Electron microscopy of cultured chromaffin cells. Chromaffin cells from *Snap-25 -/-* (E18) mice were plated on rat tail type 1 collagen-coated coverslips (Cellocate, Eppendorf, Germany) and infected (DIV2, 2 days *in vitro*) with SFVs expressing either SN25B wild type or SN25B mutants harboring single (M71A or I192A) or double (M71A, I192A) mutations in layer +5. Cells were fixed for 45 min at room temperature with 2.5% glutaraldehyde in 0.1 M cacodylate buffer (pH 7.4), washed, embedded and analyzed as before (*S9-S11*). Analysis of secretory vesicle distribution was done blinded for the experimental condition. Docked vesicles were without any measurable distance between granule and plasma membrane.

Supporting text

The rosette model of SNARE-complexes

We wish to arrive at a mathematical expression for the expected secretion when two different SNARE species are incorporated into a rosette-like fusion complex driving secretion, and to establish a way to determine *n*, the number of SNARE-complexes in a rosette.

Assume we have two forms of SNAP-25, one at concentration $[S_1]$, which is functional, another one at concentration $[S_o]$, which is mutated and let x be the mole fraction of the mutant ($x = [S_o]/([S_1]+[S_o])$). We further assume that S_0 and S_1 forms compete for forming individual SNARE-complexes, and that they have affinity K towards some acceptor complex A.

$$A + S_0 \rightleftarrows AS_0 \qquad [AS_0] = K[A][S_0]$$

$$A + S_1 \rightleftarrows AS_1 \qquad [AS_1] = K[A][S_1]$$

We assume that a functional release apparatus is made up of *n* SNARE-complexes, possibly arranged in a rosette-like manner, and that AS_0 and AS_1 participate in such rosettes in proportion to their abundance. Then, the probability P_0 and P_1 that a given slot is filled with wildtype and mutant forms of SNARE-complexes, respectively, can be calculated according to

$$\frac{P_o}{P_1} = \frac{[S_o]}{[S_1]}; \qquad P_o + P_1 = 1;$$

yielding

$$P_1 = \frac{[S_1]}{[S_o]+[S_1]}; \quad P_o = \frac{[S_o]}{[S_o]+[S_1]} = x$$

Thus, P_0 is equal to the mole fraction of the mutant. The probability P_n that all of the *n* SNARE complexes in the rosette are occupied by S_1 (or else, that the complex is fully functional and displays wildtype kinetics):

(1) $$P_n = (P_1)^n = \left(\frac{[S_1]}{[S_o]+[S_1]} \right)^n = (1-x)^n$$

If the amplitude of the response Y (or else the amplitude of the component with wildtype kinetics) is assumed to be proportional to P_n, then

$$\text{Log Y} = \text{constant} + n \log (1-x)$$

In this case, the slope of a plot of log *Y* versus *x* is:

(2) $$\frac{d \log Y}{dx} = -\frac{n}{1-x}$$

which for $x<<1$ reduces to $-n$.

For differential affinities of species S_o and S_1 towards the acceptor complex A, with α representing the ratio of affinity constants, a similar derivation yields $-n\alpha$ for the limiting slope in such a plot.

Thus the stoichiometry of the rosette (*n*) can be found by plotting the logarithm of the response size against *x*, the mol fraction of the mutation. The slope of the plot at low x-values will be $-n$ scaled by the relative affinities of the two SNARE species towards the assumed receptor *A*. In case the mutant SNARE-form (with concentration S_o) is not an absolute dominant-negative, such that secretion is still possible when one or more mutants are incorporated into the rosette, estimation of *n* is still possible using the same expressions, if the amplitude of unperturbed secretion can be identified and used in the place of *Y* (for instance if incorporation of one mutant molecule results in a detectable kinetic change of secretion).

Supporting Figures

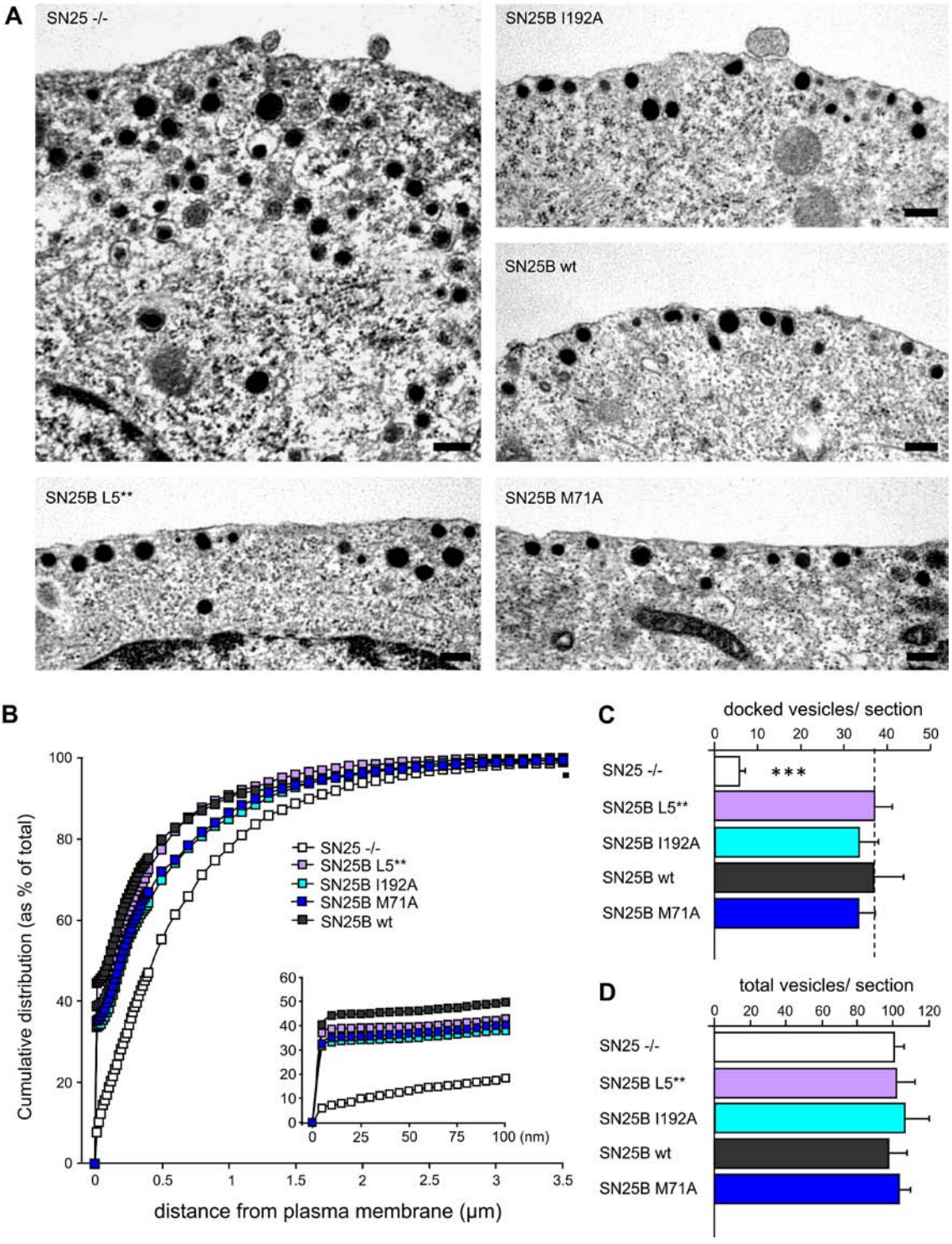

Fig. S1. Mutations interfering with Layer +5 do not compromise vesicle docking. *(A)* Electron micrographs from cultured *Snap-25* deficient chromaffin cells either untransfected (SN25 -/-) or expressing either wildtype SN25B or SN25B mutants harboring single or double mutations in layer +5. All constructs were N-terminally fused to EGFP with the exception of SN25BL5**, which was tagged with mCherry. Scalebars: 200 nm. *(B)* Normalized cumulative distribution of vesicles as a function of distance from the plasma membrane. Inset shows cumulative vesicle distribution in the sub-membrane region within 0–100 nm. *(C)* Number of docked vesicles per section (mean±SEM). *(D)* Total number of vesicles per section. For each condition 20 cells (n) and 5 animals (N) were analyzed in a blind fashion; data are means±SEM.

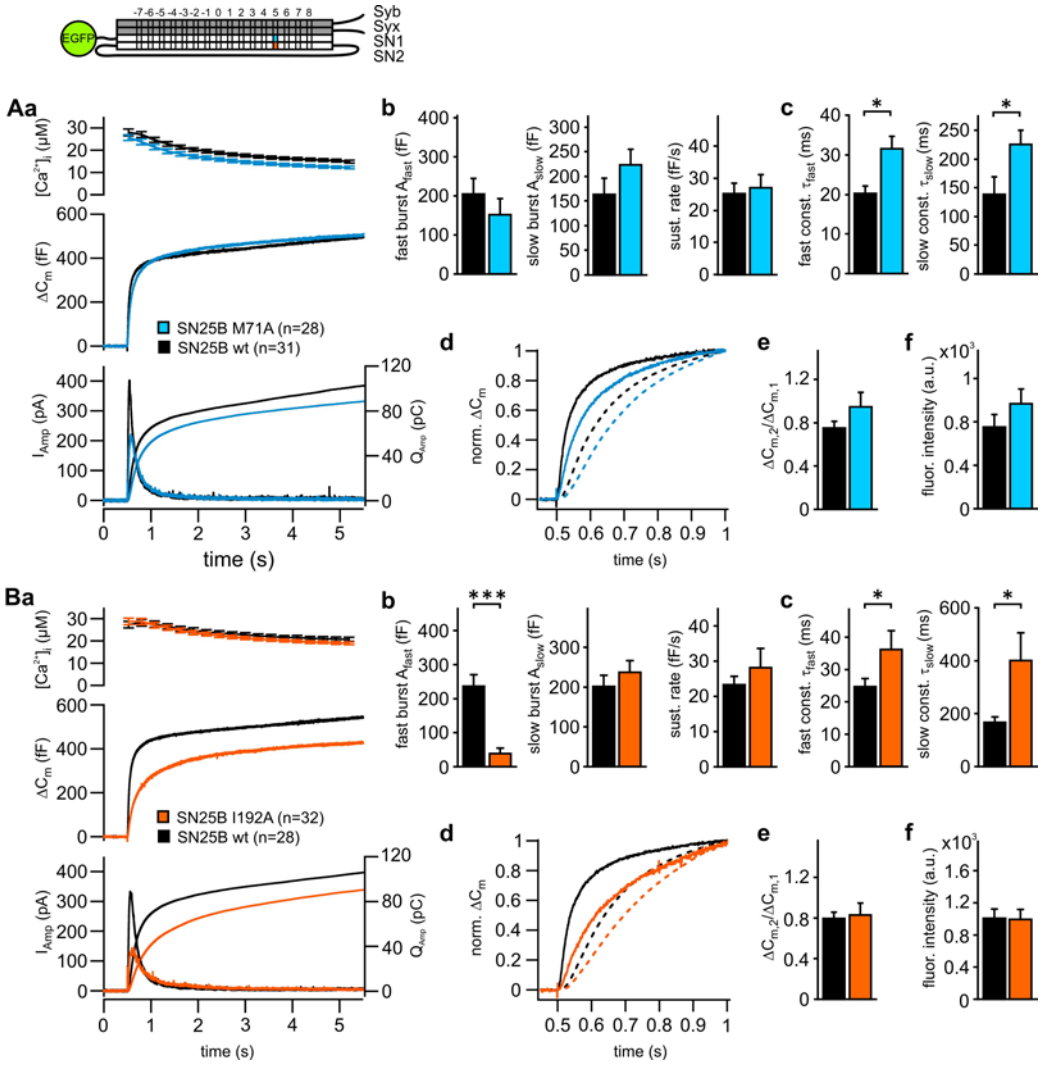

Fig. S2. Single alanine substitutions in layer +5 slow down dense-core vesicle release, but cause little inhibition of overall secretion. *Top panel:* Illustration of the position of both single amino acid exchanges. M71A is marked in blue; I192A is labeled in orange *(Aa)* Averaged data for *Snap-25* deficient chromaffin cells expressing wildtype EGFP-SN25B (SN25B wt, black, n = 31 cells) or GFP-SN25B-M71A (SN25BM71A, blue, n = 28). *Upper panel:* intracellular calcium concentration (mean ± SEM). *Middle panel:* averaged capacitance change obtained after calcium-uncaging. *Lower panel:* averaged amperometric current (thick lines, left axis) and cumulative amperometric charge (thin line, right axis). *(Ab, Ac)* The kinetic analysis of capacitance changes in SN25BM71A expressing cells

demonstrated significantly ($p<0.05$) increased fast and slow time constants, but no significant changes of the fast and slow burst amplitudes or the sustained release rate. The data are given as mean±SEM *(Ad)* Averaged capacitance change (solid lines) and cumulative amperometric charge (dashed lines) after normalization to highlight the slowdown of secretion mediated by SN25BM71A. *(Ae)* Recovery ($\Delta C_2/\Delta C_1$) of vesicle pools (mean±SEM) was assayed by applying a second flash 100 s later. *(Af)* Protein expression (mean±SEM) of both SNAP-25 variants as estimated by the intensity of their EGFP-tags. *(B)* Analysis of secretion in SNAP-25 deficient cells expressing SN25BI192A (SN25B I192A, orange, n = 32) compared to wildtype EGFP-SN25B (SN25B wt, black, n = 28). For an explanation of panels, see legend to A. *(Ba)* Mean secretion was reduced, and release was slowed down. *(Bb, Bc)* Fast and slow time constants (mean±SEM) were significantly ($p<0.05$) prolonged, and the amplitude of the fast burst (mean±SEM)was strongly depressed ($p<0.0001$). Sustained release was unchanged. *(Be)* Recovery and *(Bf)* protein expression (mean±SEM) were comparable to controls.

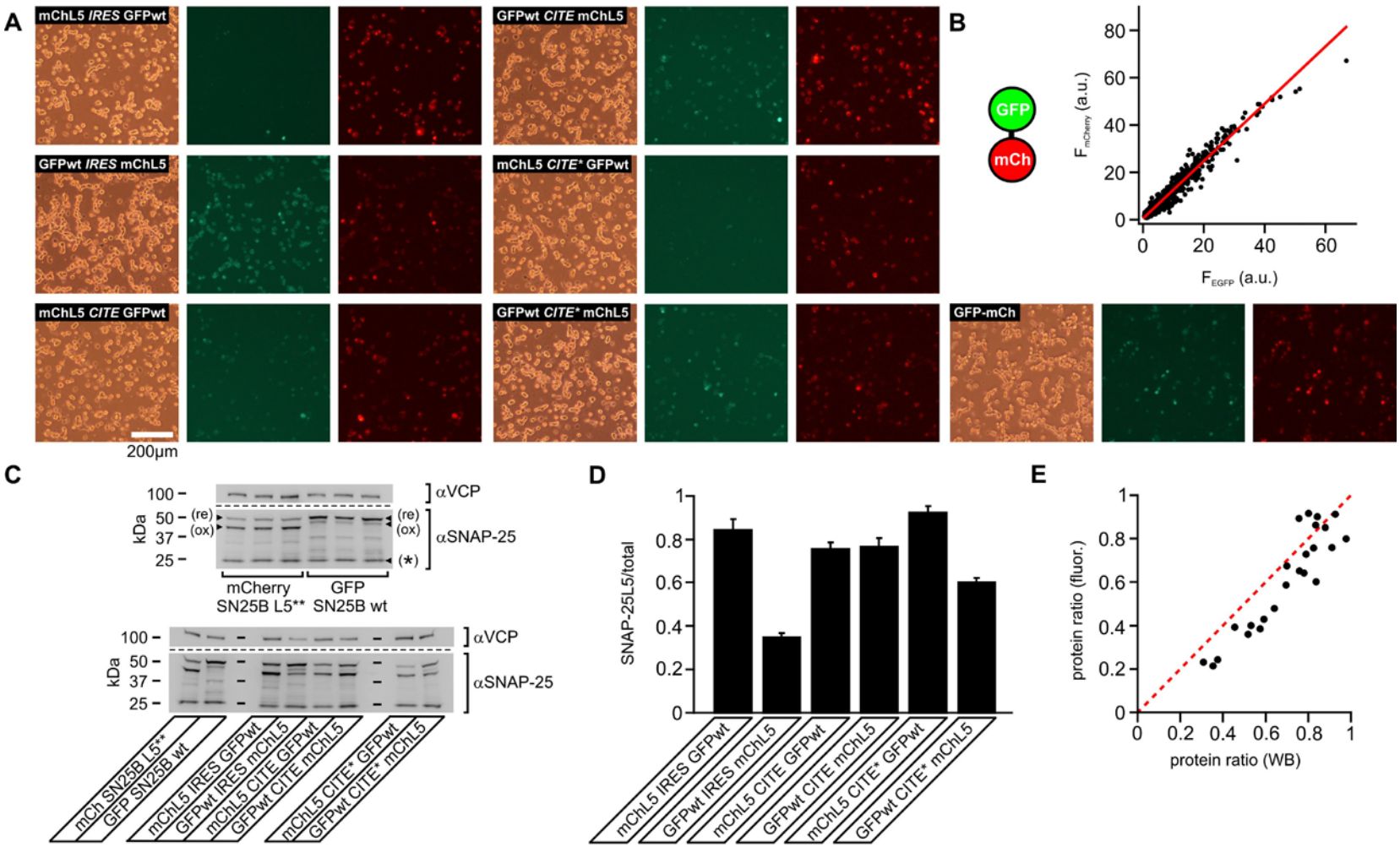
A
mChL5 IRES GFPwt
GFPwt CITE mChL5
GFPwt IRES mChL5
mChL5 CITE* GFPwt
mChL5 CITE GFPwt
GFPwt CITE* mChL5
GFP-mCh
200µm
B
GFP
mCh
F_mCherry (a.u.)
F_EGFP (a.u.)
C
kDa
100
50
37
25
(re)
(ox)
(*)
αVCP
αSNAP-25
mCherry SN25B L5**
GFP SN25B wt
mCh SN25B L5**
GFP SN25B wt
mChL5 IRES GFPwt
GFPwt IRES mChL5
mChL5 CITE GFPwt
GFPwt CITE mChL5
mChL5 CITE* GFPwt
GFPwt CITE* mChL5
D
SNAP-25L5/total
E
protein ratio (fluor.)
protein ratio (WB)

Fig. S3 Characterization of bicistronic Semliki Forest viruses. *(A)* Microphotographs of cultured bovine chromaffin cells infected with bicistronic Semliki Forest (SF) viruses expressing both mCherry-SN25BL5** (mChL5) and wildtype EGFP-SN25B (GFPwt). Each panel contains a transmission (*left*), EGFP fluorescence (*middle*), and mCherry fluorescence (*right*) image. The corresponding virus type is indicated on top of each panel. *(B)* Virally expressed EGFP-mCherry fusion protein was used as a reference for calculation of the fraction of mCh-SN25BL5** expression. *Lower panel*: Transmission image (*left*), EGFP fluorescence (*middle*), mCherry fluorescence (*right*). *Upper panel:* A plot of the EGFP- versus mCherry fluorescence intensity demonstrates a constant intensity ratio for equimolar amounts of EGFP and mCherry fluorophors (*upper panel*), which was used to determine a constant for transforming intensity ratios into protein ratios. (*C*) Western blot analysis of bovine chromaffin cells following infection by viruses. mCherry-tagged and EGFP-tagged SNAP-25 exhibits differential formation of oxidized species under non-reducing Western blot conditions (*upper panel*). Reduced SNAP-25 variants are marked “re”; oxidized species are labeled as “ox”. Untagged, endogenous protein is indicated by “*”. Note the constant ratio of oxidized and reduced species within three independent samples for mCh-SN25BL5** and EGFP-SN25B. The lower panel depicts a blot of lysates obtained from bovine chromaffin cells infected with six different dicistronic SF viruses. Valosin–containing protein (VCP) was used as loading control in all Western Blot experiments. *(D)* Quantification of Western blot data (three sets of independent samples), given as mean±SEM. *(E)* Comparison of Western blot data and fluorescence intensity measurements. Each data point in the plot represents analysis results derived from the same sample of cultured bovine chromaffin cells. An ideal correlation of data from both analyses methods would place data points on the dashed identity line.

Given the semi-quantitative nature of Western blot data, results obtained by both methods are well matched.

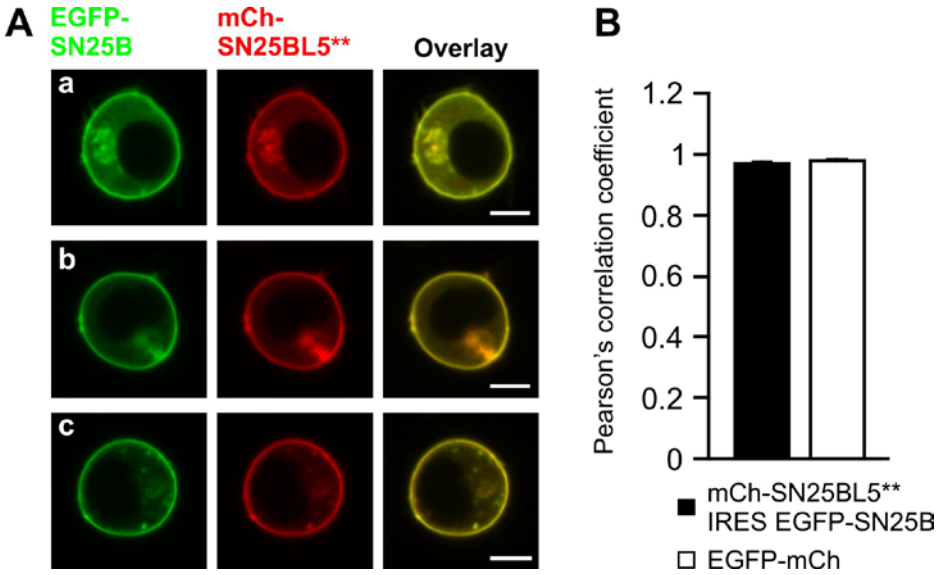

Fig. S4 Cellular distribution of mutant SNAP-25 is indistinguishable from wildtype protein. *(A)* Example microphotographs of cultured mouse chromaffin cells co-expressing mCh-SN25BL5** and EGFP-SN25B (a-c). In each panel left images depict EGFP fluorescence (green), middle images show mCh fluorescence (red), and right pictures present the overlay of both signals. Note that intracellular aggregation of virally expressed protein can vary between cells. The expression pattern of mCh-SN25BL5** overlapped with EGFP-SN25B. *(B)* Colocalisation was quantified based on Pearson's correlation coefficient. For mCh-SN25BL5** and EGFP-SN25B Pearson's coefficient was near 1 (0.970±0.004; n=46) indicating strong colocalisation of both proteins. EGFP-mCh fusion protein was used as reference and yielded a comparably high Pearson's coefficient (0.978±0.005; n=17). Data are given as mean±SEM.

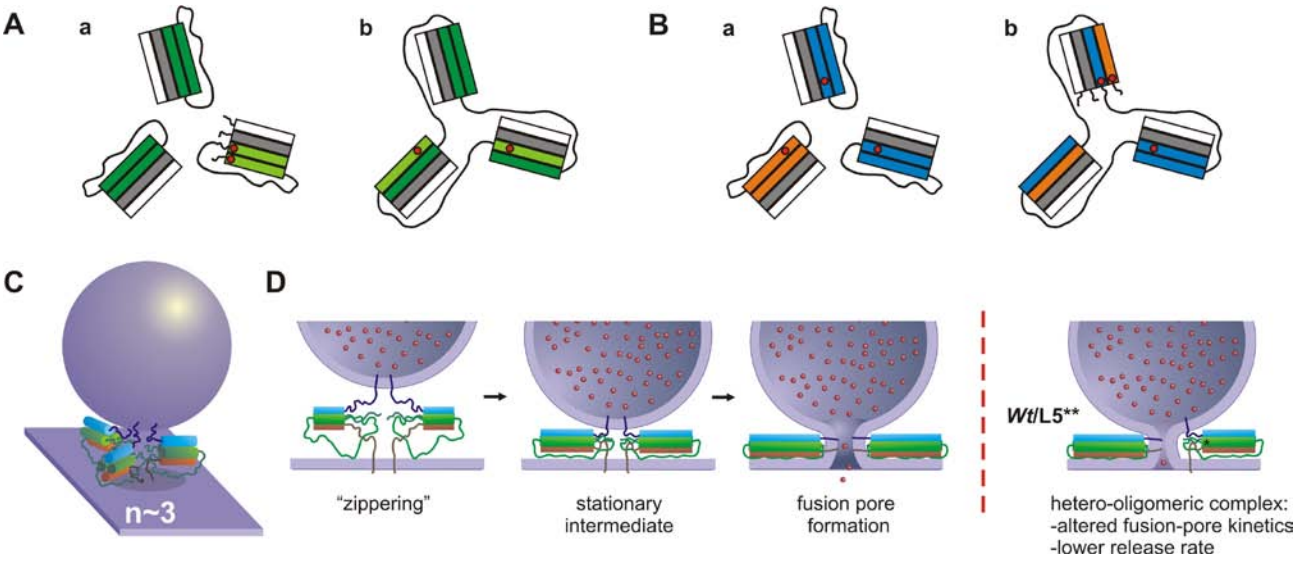

Fig. S5 Schemes of fusion. *(A)* Incorporation of SN25BL5** in rosettes together with wildtype protein separates the single mutations (red dots) if domain-swapping occurs (b), whereas in the absence of domain-swapping (a), the two single mutations always join the same SNARE-complex. *(B)* Test of domain-swapping hypothesis: coexpression of the two single mutations (M71A and I192A) in the presence of domain-swapping (b) regenerates the catastrophic SN25BL5** mutation in some SNARE-complexes, whereas if domain-swapping does not occur, the single mutations always stay separate (a). The experiments presented in Fig. 4 in the main manuscript argue against domain-swapping. *(C)* Cartoon showing three SNARE-complexes mediating fast vesicle fusion. *(D)* The 'zippering' of the SNARE complexes pulls both membranes together and is followed by fusion pore formation and full fusion. Right panel: SN25BL5** probably reaches the intermediate state normally, but possesses a defect in the assembly of the C-terminal end of the complex and therefore cannot contribute to final fusion. Heteromeric rosettes are characterized by lower fusion rates and altered amperometric spike waveform.

Supporting references

S1. J. B. Sorensen *et al.*, *Cell* **114**, 75 (Jul 11, 2003).

S2. I. Delgado-Martinez, R. B. Nehring, J. B. Sorensen, *J Neurosci* **27**, 9380 (Aug 29, 2007).

S3. N. C. Shaner *et al.*, *Nat Biotechnol* **22**, 1567 (Dec, 2004).

S4. J. B. Sorensen *et al.*, *Proc Natl Acad Sci U S A* **99**, 1627 (Feb 5, 2002).

S5. Y. A. Bochkov, A. C. Palmenberg, *Biotechniques* **41**, 283 (Sep, 2006).

S6. G. Nagy *et al.*, *J Neurosci* **22**, 9278 (Nov 1, 2002).

S7. J. B. Sorensen *et al.*, *Embo J* **25**, 955 (Mar 8, 2006).

S8. S. Bolte, F. P. Cordelieres, *J Microsc* **224**, 213 (Dec, 2006).

S9. R. F. Toonen *et al.*, *EMBO J.* **25**, 3725 (Aug 23, 2006).

S10. H. de Wit *et al.*, *Cell* **138**, 935 (Sep 4, 2009).

S11. H. de Wit, L. N. Cornelisse, R. F. Toonen, M. Verhage, *PLoS ONE* **1**, e126 (2006).